Paper 78

Proceedings of the Eighth International Conference on Engineering Computational Technology,
B.H.V. Topping, (Editor),
Civil-Comp Press, Stirlingshire, Scotland

A Numerical Approach to the Effect of Surface Texturing on Parallel Thrust Bearings

F. Abate, V. D'Agostino and R. Di Giuda
Department of Industrial Engineering
University of Salerno, Fisciano (SA), Italy

Abstract

Numerous recent studies have considered the modelling of lubricant flow in micro-textured configurations and they have shown that the surface texturing technique can generate a load carrying capacity even between two parallel surfaces of a thrust bearing.
The aim of this paper is to provide an effective numerical tool to examine how texture might influence on tribological characteristics in mixed lubrication regime through a parametric analysis.
The present theoretical model considers dimples all having same width and depth for each simulation. The influence of texture depth and texture density are investigated. A numerical study of a thrust bearing with a series of dimples created on the stationary surface is carried out in order to evaluate the influence of the texture parameters. Simulations were performed varying the parameters of, width, depth and density of the dimples. The obtained results are presented in terms of pressure distribution, friction coefficient, minimum film thickness and load carrying capacity.

Keywords: parallel thrust bearing, surface texturing, friction coefficient.

1 Introduction

Theory of hydrodynamic lubrication yields linear velocity distribution with zero pressure gradients between smooth parallel surfaces under steady state sliding. This results in an unstable hydrodynamic film that would collapse under any external force acting normal to the surface.
However, in practical, stable lubricating films can develop between parallel sliding , generally because of some mechanism, which relaxes one or more of the assumptions of the classical theory.
Stable fluid can be obtained with macro or micro surface structure of different types. In particular, some authors [1-3], have shown that the presence of an inlet zone

having tailored roughness can provide load carrying capacity in parallel sliding. Tonder [4-5] pointed out that introducing a series of dimples or roughness at the inlet of a sliding surface contact can generate extra pressure and thus support higher load. In the same way, laser textured surface (LST), well known technology emerged in the last decade as a viable option of surface engineering, can generate a load carrying capacity even between two parallel surface. For this reason texturing have already been a subject of several theoretical and experimental which have shown that texturing to be an effective method for improving the tribological performance of lubricated interfacing surfaces. In fact, it has been demonstrated that a significant improvement in load-carrying capacity, wear resistance, friction coefficient of tribological components can be obtained by forming reasonable surface textures on their surfaces. The mechanisms of improvement can be explained as follows: serving as a micro - hydrodynamic bearing in cases of full or mixed lubrication to generate additional hydrodynamic pressure to increase the load-carrying capacity; acting as micro- reservoirs for lubricant in cases of starved lubrication conditions; trapping debris to prevent severe wear on the surfaces.
Among these mechanisms, generating additional hydrodynamic pressure is usually considered as the most significant effect of surface texture under low-load and high-speed conditions, so that it has drawn much more focused attention.
Furthermore, this technology is extremely fast, clean to the environment, and provides excellent control of the shape and size of dimples that allows realization of optimum parameters.
Thus, in order to maximize the texture effect on the tribological performance, a great deal research has been carried out.
A fundamental work on LST is carried out at Argonne National Laboratory in the USA. The effect of LST on the transition from boundary to hydrodynamic lubrication regime was experimentally investigated [5] by measuring friction and electrical-contact resistance in a pin-on-disk unidirectional sliding conformal contact. LST was observed to expand the range of the hydrodynamic lubrication regime in terms of load and sliding speed. Furthermore, LST was observed to reduce the friction coefficient substantially under similar operating conditions when compared with untextured surfaces.
In bibliography, two solutions of LST are presented: the dimples may be repeated over the entire surface area or on a part. The results shown that full texturing seems be unable to generate hydrodynamic lift in parallel sliders, on the contrary, partial texturing appears capable to generating substantial load carrying capacity useful for finite and generates sliders [6-8] .
Investigations of this aspect was also of interest for reciprocating automotive components; the laser surface texture, in fact, may provide oil retention capability that will protect the sliding surfaces against seizure [9].
In this context, this paper aims to provide an effective numerical tool to examine how texture might influence on tribological characteristics in mixed lubrication regime through a parametric analysis. The main goal of this numerical study in the present work is to investigate the influence of the Partial LST on a tribological performance of finite parallel thrust bearing and searching for a geometric optimal configuration of the textured pad portion.

2 Theoretical Model

A simplified geometrical model of a single pad in the form of a rectangular parallel slider is considered in this paper and displayed in Figure 1.
It is well known, in fact, that each pad, when properly textured, develops the same hydrodynamic force. Hence, in order to evaluate the load carrying capacity of the complete parallel thrust bearing it is sufficient to determine the hydrodynamic pressure distribution over a single pad.

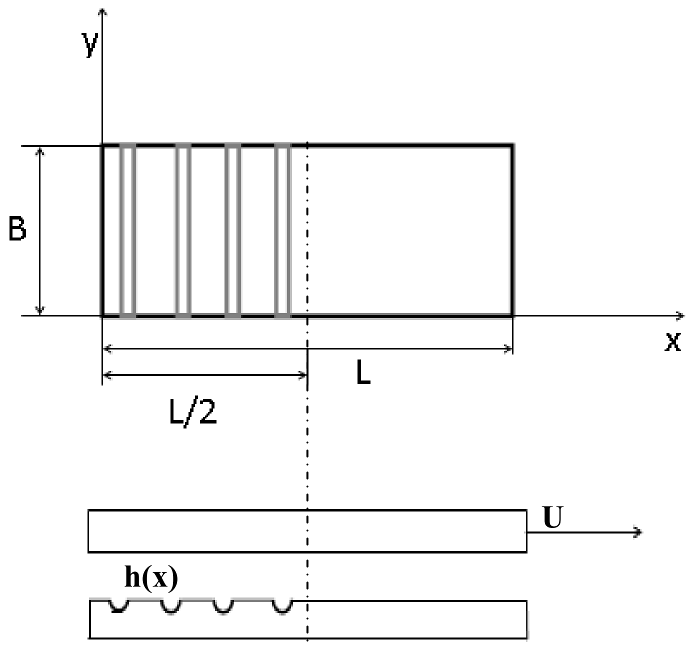

Figure 1: Schematic representation of a partially laser textured parallel slider

The dimples are uniformly distributed over the half-width, L/2, of the pad in the sliding direction, x, with a distance d_d function of a number, depth(h_d) width(w_d)of texture dimples and length of the pad chosen. The texture consists of a system of equal dimples having sinusoidal profile, expressed mathematically as follows:

$$h(x) = h_d\left[\cos\left(\frac{x - x_{in}}{x_{out} - x_{in}}\right)2\pi - 1\right] \tag{1}$$

Then, the film thickness, *hf*, will be the sum of two components:

$$h_f = h_0 + h(x) \tag{2}$$

where h_0 is the minimum film thickness and *h(x)*, the function described above.
A merit of this paper is to consider the value of h_0, not as a given input, but like an output of the sum of loads acting on the pad, as shown below.

2.1 Governing equation

The Reynolds equation in two-dimensional form, applied to problems in finite geometry, does not admit exact solution analytically, but requires a resolution of numeric type. Moreover, obtaining the solution is further complicated by the equation of balance of the loads arising from both the fluid and the contacts multi asperities. Furthermore, the discretization carried out with fixed grid has led to a high value of nodes, in order to reconstruct with accuracy the pressure distribution that are carried inside the cavities. The numerical solution of the problem has been addressed on the computational domain, **Ω**, represented by a finite number of points (xi, zj) of the physical domain. The two-dimensional, steady-state form of the Reynolds equation for an incompressible Newtonian fluid in a laminar flow is given by:

$$\frac{\partial}{\partial x}\left(\frac{h^{3}\rho}{\mu}\frac{\delta p}{\delta x}\right)+\frac{\partial}{\partial z}\left(\frac{h^{3}\rho}{\mu}\frac{\delta p}{\delta z}\right)=6U\frac{\delta(\rho\, h)}{\delta x} \tag{3}$$

where x and z are the Cartesian coordinates, parallel and normal to the sliding direction, respectively, *h* and *p* are the local film thickness and the pressure at a specific point of the slider, respectively. In order to reduce Equation (3) to a dimensionless form, the following dimensionless parameters are introduced:

$$x^*=\frac{x}{L} \qquad z^*=\frac{z}{L} \qquad h^*=\frac{h}{h_{rif}} \qquad p^*=\frac{p}{h_{rif}} \qquad \mu^*=\frac{\mu}{\mu_0} \qquad \rho^*=\frac{\rho}{\rho_0} \tag{4}$$

with:

$$p_{rif}=\frac{6\mu_0 UL}{h_{rif}^{\ 2}} \tag{5}$$

The dimensionless form of Reynolds Equation becomes:

$$\frac{\partial}{\partial x}\left(\frac{h^{*3}\rho^*}{\mu^*}\frac{\delta p^*}{\delta x^*}\right)+\left(\frac{1}{\lambda^2}\right)\frac{\partial}{\partial z^*}\left(\frac{h^{*3}\rho^*}{\mu^*}\frac{\delta p^*}{\delta z^*}\right)=\frac{\delta\rho^* h}{\delta x^*} \tag{6}$$

where :

$$\lambda=\frac{B}{L} \tag{7}$$

The boundary conditions, expressed on the inside domain, are zero relative pressure:

$$p(x,z)=0\, for(x,z)\in\partial\Omega \tag{8}$$

The Reynolds equation can provide negative pressure values. These values, however, are not physically acceptable, since in such circumstances, the fluid evaporates being the absolute pressure limited by the value of the vapor pressure, next to the atmospheric pressure. The process just described, said cavitation, must be taken into account in solving the Reynolds equation. There are several methods to model this phenomenon. The most immediate, but also less accurate, is known as Half Sommerfeld condition or Gumbel that is to solve the equation on the whole domain and then impose zero any negative values. This method, however, does not guarantee that the continuity equation, on which the same Reynolds equation is based, is observed everywhere. In this work was taken into account a condition more accurate; this is called the Reynolds condition, which requires that the pressure goes to zero together with its derivative, verifying, thus, the continuity equation. The algorithm, consisting in changing equal to zero the values of negative pressure not just be computed, allows the emergence directly the border between the area of positive pressure and the cavitation zone; the pressure distribution obtained also satisfies the condition Reynolds.

2.2 Load sharing concept

In mixed lubrication, the external load is supported both by the hydrodynamic component and the component caused by the multi asperity contact. Then, the friction coefficient will be given by the ratio between the total friction force, F_t ,and the total load Wt.:

$$f = \frac{F_t}{W_t} = \frac{(F_L + F_A)}{(W_L + W_A)} \tag{9}$$

With regard to the problem related to the contact between the surface roughness and thus the calculation of W_A and F_A, in this work is used the model of Greenwood and Tripp.

This model assumes that the contacting surfaces are both rough and that the parameters characterizing the surface topography are the same for both bodies. Under these assumptions the contact pressure is expressed, in its form dimensional by:

$$p_c(x, y) = \frac{6\sqrt{2}}{15}(n\vartheta\sigma)^2 E' \sqrt{\frac{\sigma}{\vartheta}} \tilde{F}_{5/2}\left(\frac{h(x, y)}{\sigma}\right) \tag{10}$$

where n is the density of the roughness, β the mean radius of the individual asperities, σ the standard deviation of the distribution of peaks and finally E' is the modulus of elasticity equivalent calculated as :

$$E' = \frac{1}{2}\left(\frac{1-\nu_1^{\,2}}{E_1} + \frac{1-\nu_2^{\,2}}{E_2}\right) \tag{11}$$

where E, ν indicate the Young's modulus and Poisson's ratio of the bodies in the pair. The function $\tilde{F}_j$ is defined by:

$$\widetilde{F}_j\left(\frac{h}{\sigma}\right)=\int_{h/\sigma}^{\infty}\left(s-\frac{h}{\sigma}\right)^j\phi(s)ds \tag{12}$$

in which $\phi(s)$ is the probability density function referred to the top of the surface asperities. Most of the mechanical machining gives rise to a surface finish for which it is possible to assume a Gaussian distribution of the top; in this case the probability function is expressed by:

$$\phi(s)=\frac{1}{\sqrt{2\pi}}e^{-\frac{s^2}{2}} \tag{13}$$

Then integrating the pressure on actual contact is possible to obtain the total load W_A and therefore the frictional force F_A:

$$F_A=\tau_0 A_c+aW_A \tag{14}$$

where a is the coefficient of dry friction between the bodies, τ_0 is the shear stress of the material and A_c is the area of real contact, calculated as:

$$A_c=(\pi n\vartheta\sigma)^2 A_n\widetilde{F}_2\left(\frac{h}{\sigma}\right) \tag{15}$$

being A_n the nominal area of contact.

2.3 Balance equations

The equilibrium condition requires that the total load acting on the slider is equaled by the total load capacity, given by the sum of the fluid-dynamic loads and by contact. The equilibrium equation, therefore, is given by:

$$W=W_L+W_A \tag{16}$$

The hydrodynamic load is given by the integral numerical extended to the domain Ω of solution of the hydrodynamic pressure calculated using the equation of Reynolds; the load from the contact is calculated through the integration of the contact pressure is obtained by the model of GT:

$$W_L = \iint_{\Omega} \tilde{p}_L(\tilde{x}, \tilde{y}) d\tilde{x} d\tilde{y} \tag{17}$$

$$W_A = \iint_{A_C} \tilde{p}_C(\tilde{x}, \tilde{y}) d\tilde{x} d\tilde{y} \tag{18}$$

The dimensionless form of aerodynamic frictional force aerodynamic is calculated through the integration of the effort viscous shear τ:

$$\tau = 3\tilde{h} \frac{\delta \tilde{p}_L}{\delta \tilde{x}} + \frac{\tilde{\mu}}{\tilde{h}} \tag{19}$$

Integrating (2.39) over the entire domain Ω by the frictional force fluid is obtained:

$$\tilde{F}_L = \iint_{\Omega} \tilde{\tau}(\tilde{x}, \tilde{y}) d\tilde{x} d\tilde{y} \tag{20}$$

3 Numerical procedure

The governing equations, in particular the Reynolds Equations, the multi asperity model and and the equation of load balance, are coupled by the independent variable that defines the value of separation between the surfaces in contact, h_0. Therefore, appears clear the need to implement a resolution algorithm based on an iterative loop. In particular, given an initial guess value of h_0, the algorithm proceeds by solving the hydrodynamic pressure field inside the Gauss-Seidel procedure.

Thus, obtained convergence, integrals of the hydrodynamic loads, such as numerical integral of the pressure distribution and the friction load, as a numerical integral of the shear stress distribution on fixed surface, are calculated; if the equation of balance of the loads is not met, a new value of the minimum film thickness ,through “under – relaxation γ”, is recomputed and the loop begins again. The procedure just described is shown schematically in Figure 2.

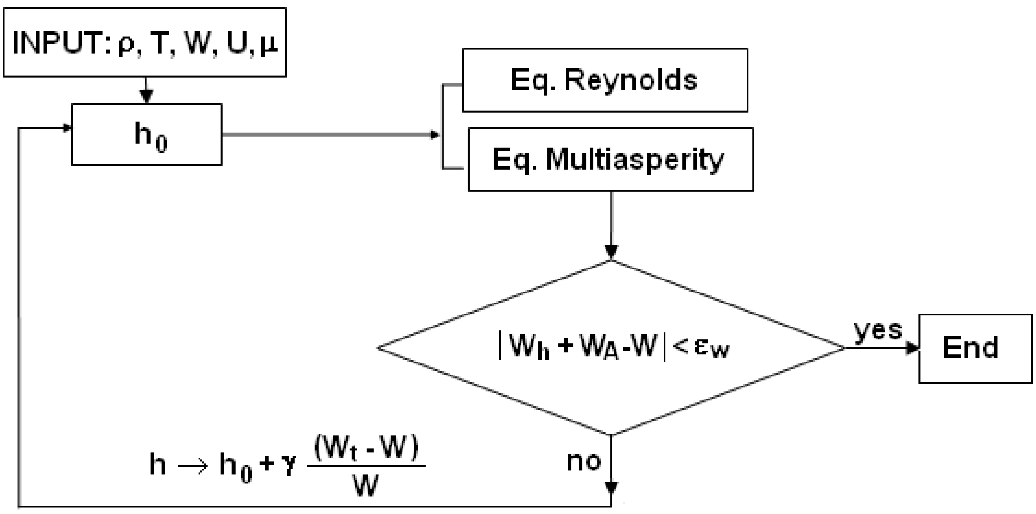

Figure 2: Gauss-Seidel procedure

4 Results and discussion

A parametric analysis was performed to investigate the effect of various parameters of the problem on the load carrying capacity and friction coefficient. Simulation parameters are listed in Table 1.

Symbol	Description	Value	Unit
L	Pad lenght	10	mm
B	Pad wight	5÷15	mm
E	Pin Young modulus	$2.06 \cdot 10^{11}$	N m^{-2}
ν	Pin Poisson ratio	0.3	-
W	Normal load	50	N
U	Pad velocity	1÷4	m s^{-1}
p_{ref}	Hydrodynamic reference pressure	$6\,\mu_0\, U\, D\, h_{ref}^{-2}$	Pa
ρ_0	Oil ref. density	860	kg m^{-3}
μ_0	Oil ref. viscosity	0.08	Pa s
T_0	Oil avarage temperature	40	°C
n	Number of dimples	1÷8	-
w_d	Dimple wight	0.25	mm
h_d	Dimple depth	5 ÷ 15	μm
α	Textured portion of pad	0.5	
b	Asperity distribution density	$4 \cdot 10^6$	m^{-2}
ϑ	Asperity radius	1	μm
σ	Asperity standard deviation	0.55	μm
τ_0	Shear strength constant	$2 \cdot 10^6$	Pa
a	Boundary friction coefficient	0.12	-

Table 1

In agreement with other authors, two different effects of dimples were found corresponding to the cases of full texturing and partial texturing. These two different effects are demonstrated in Figures 3and 4, where the hydrodynamic pressure profile in the two cases, for the same number of dimples and other operating conditions, are shown. It has been found, by the simulations carried out, that in the case of "*Full Surface Texturing*" ($\alpha = 1$), each dimple individually contributes to the formation of a hydrodynamic pressure can support external loads; the dimples not interact (an individual dimple effect) resulting in periodic and symmetrical pressure distribution with local cavitation zones (p=0) .This phenomenon, clearly, leads to a reduced load capacity. It can, however, be beneficial in very short slider bearings as is the case with mechanical seals ,for example [7].

In contrast, in the case of "*Partial Surface texturing*"($\alpha < 1$), each dimple strongly affects its neighboring dimples (a collective dimples effect). This collective effect results in a step-like pressure distribution over the textured portion of the slider and the maximum pressure, the distribution of which is not symmetric, is obtained at the beginning of the section untextured.

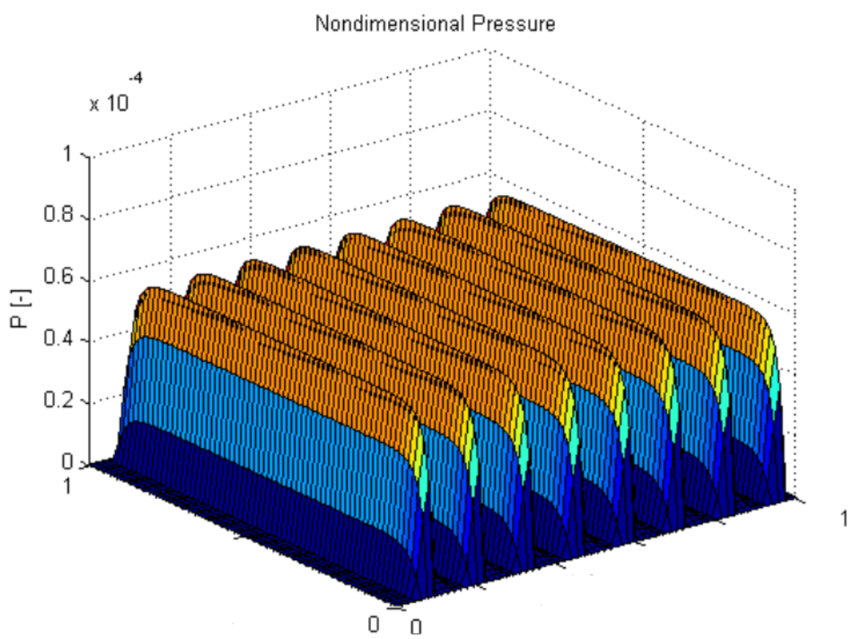

Figure3: Schematic representation of a fully laser textured parallel slider

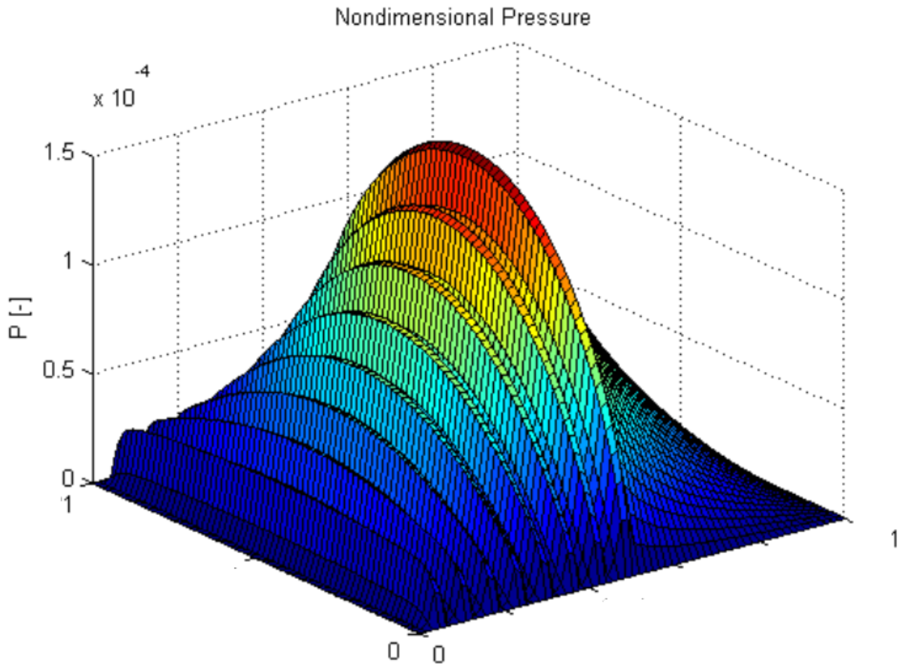

Figure 4: Schematic representation of a partially laser textured parallel slider

Then, one of the first major results obtained is that the Partial Texturing provides better performance in terms of pressure distribution, compared with Fully Texturing. Here below, some graphs, Figures 5-8, “friction coefficient vs speed” and corresponding “minimum film thickness vs. speed”; for different configurations of partial textured pad ($\alpha = 0.5$) are shown.

These profiles were obtained for a fixed value of the characteristic slider ratio B / L = 1 and of amplitude w_d, varying the number of dimples (and therefore the distance between them) and the depth. In particular, the plots are shown for a h_d of 5, 10 and 15 μm respectively. In each graph, it is also shown the tribological performance of a pad with the same geometry but without texturing (no dimples).

It may be noted that the configuration with a greater number of dimples (n = 7-8) appears to be the best, in terms of friction coefficient reduction and consequent increase of the minimum film thickness, for a depth of the single dimple $h_d \leq 10\mu m$. In fact in the graph representative of a pad with dimples uniformly distributed with a depth of 15 μm, the configuration with a smaller number of dimples behaves better than that with a greater number. This results highlight the importance of the parameter "aspect ratio", i.e. the ratio of dimple depth over dimple width. Assigned a certain number of dimples can be seen that the aspect ratio, plays a major role in affecting the tribological performance of LST components. This is because the aspect ratio defines the average slope of the converging film thickness zone of each dimple, which is known to be the main factor affecting load capacity in slider bearings.

The optimum aspect ratio changes with the number of dimples, or rather by changing the mutual distance between the same. In this model, in fact, the distance is not fixed, but varies with the number of dimples. All this results in the fact that an optimal configuration will be the result of a compromise between the optimal number of dimples, the optimal value of aspect ratio and optimal distance between the dimples. Therefore, it is possible say that with an "aspect ratio" of 0.02 the solution with 8 dimples is best in terms of friction behavior.

As expected the configuration without texturing appears to have the worst behaviour.

It is also interesting to note that the influence of the number of dimples doesn't involve an equal trend in all lubrication regimes; in the mixed regime, in fact, increasing the number of dimples, the positive contribution of these to reduce friction, increases; a reverse trend is observed in the hydrodynamic regime.

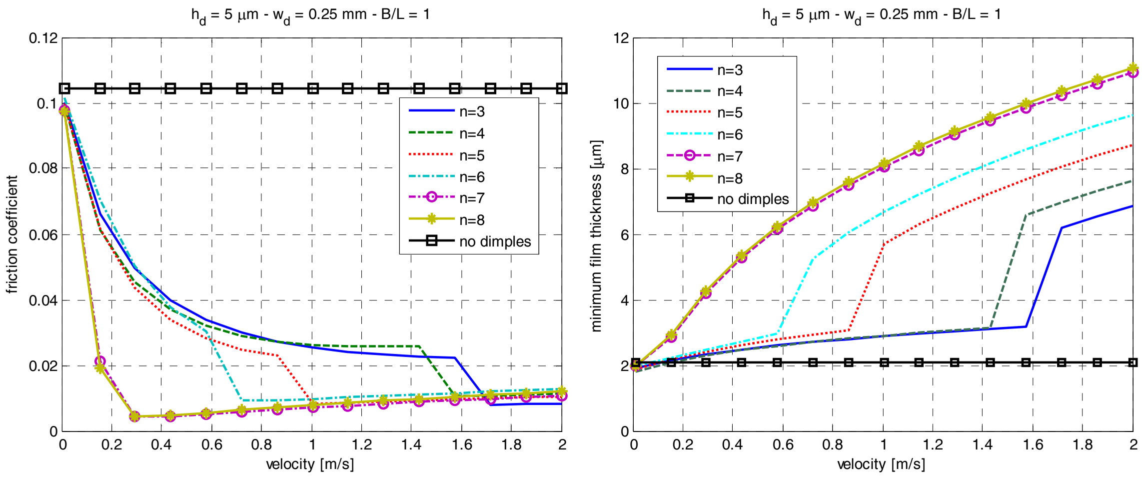

Figure 5: Friction coefficient vs velocity (a)–minimum film thickness vs velocity (b) Dimple depth $h_d = 5\mu m$

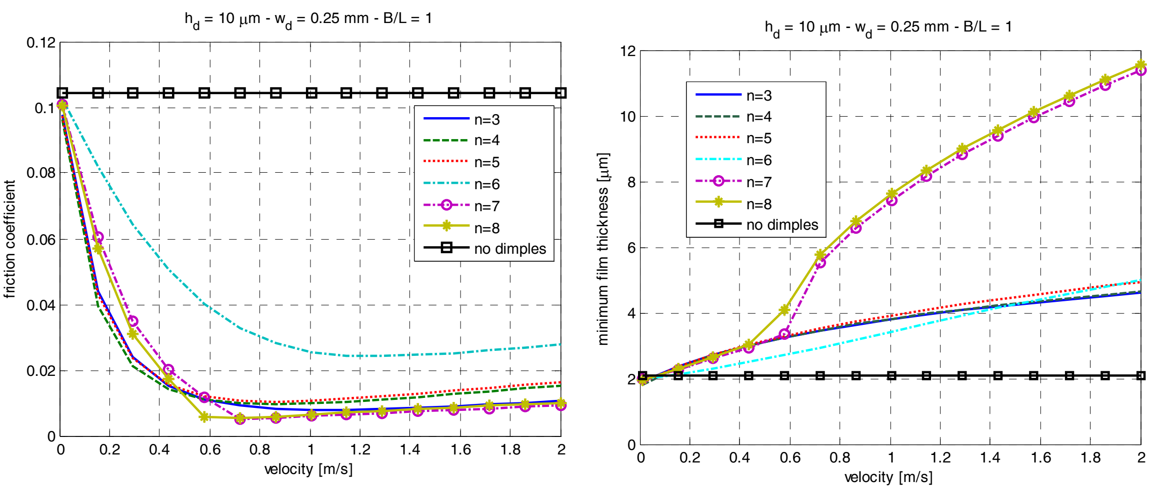

Figure 6: Friction coefficient vs velocity (a)–minimum film thickness vs velocity (b) Dimple depth $h_d = 10\mu m$

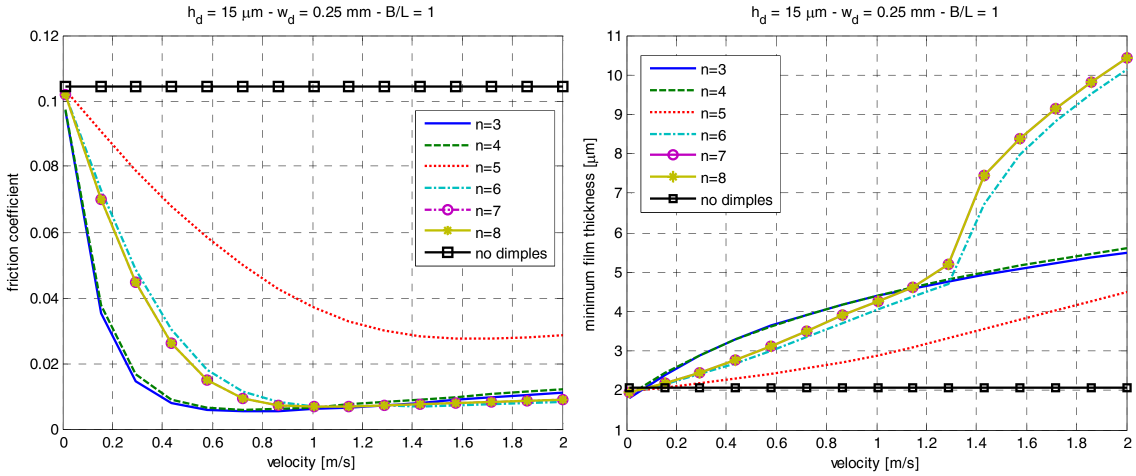

Figure 7: Friction coefficient vs velocity (a)–minimum film thickness vs velocity (b)
Dimple depth $h_d = 15\mu m$

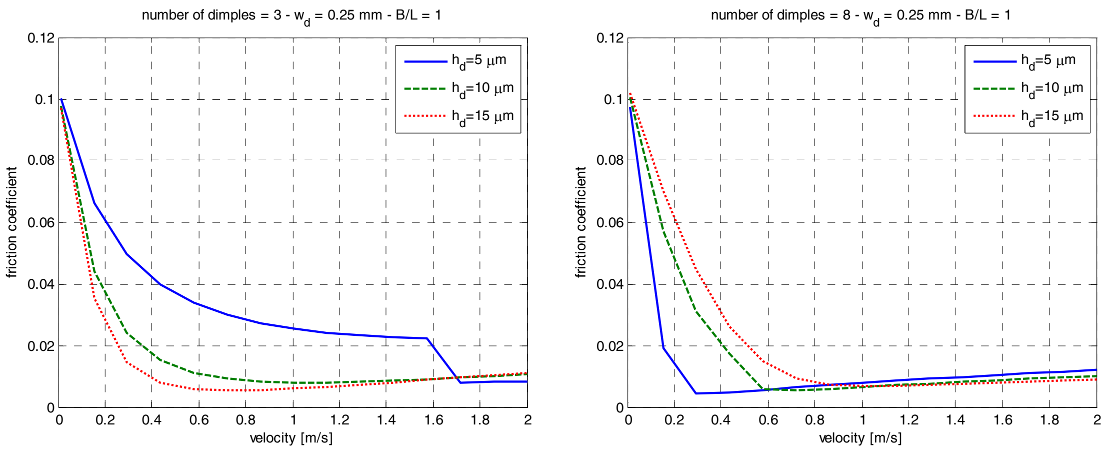

Figure 8: Friction coefficient vs velocity for 3 dimples(a) and for 8 dimples (b)

In Figure 9 (a) the trends of the fluid film load capacity and asperities load capacities are shown. It is noted that, increasing the number of dimples, the rate due to the fluid capacity is greater than that due to asperities; this explains the decrease of the friction coefficient increasing the number of dimples.
In Figure 9 (b) the influence of number of dimples on fluid load capacity both PLT and FLT is shown.

In both cases it is noted the existence of an optimum value for the number of dimples after which do not have then further improvements.

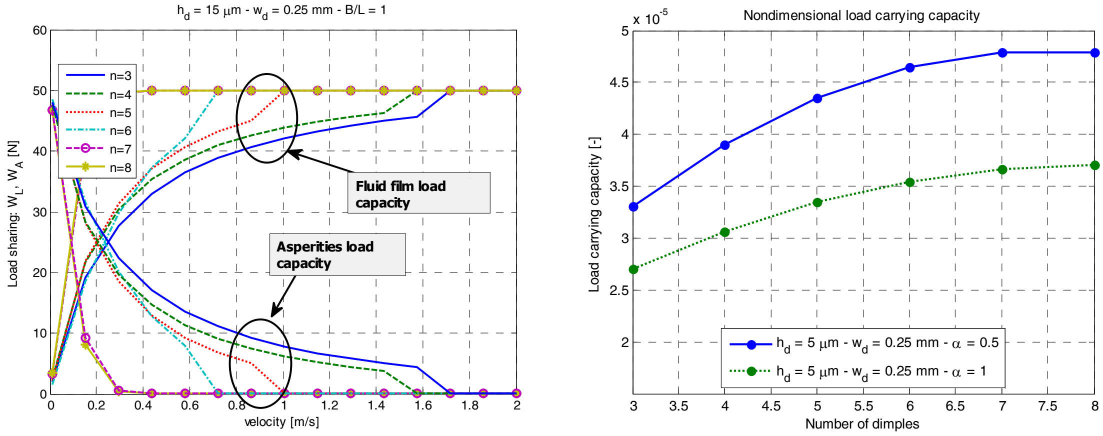

Figure 9: The effects of number of dimples and velocity on the load sharing (a) and fluid load capacity with dimples number (b)

Finally, in Figure 10 is shown a graph showing how the presence of the slots is more relevant in the case in which slider ratio is greater than or equal to 1.

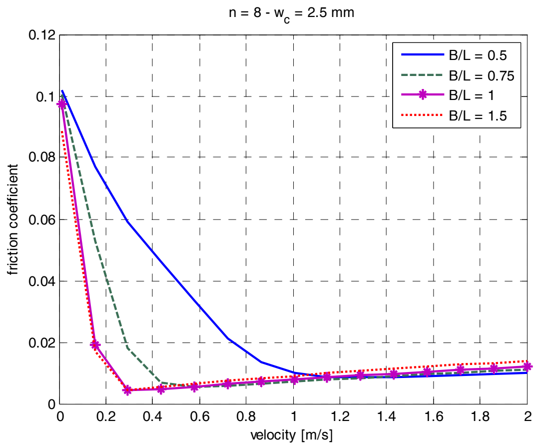

Figure 10: Friction coefficient vs velocity for different B/L values

5 Conclusion

A theoretical model was developed to analyse the potential of LST in parallel bearing lubrication. The effect of surface texturing on lubrication regime transitions from mixed to hydrodynamic was studied by measuring friction coefficient, minimum film thickness and load carrying capacity. The main conclusions can be drawn are:

- the partial laser texturing (PLT) seems to be much more suitable than the full laser texturing (FLT) to the formation of a pressure that can support external loads;

- the existence of dimples on steel surface was observed to reduce the friction coefficient substantially, when compared with un - textured surfaces;
- the positive effect of the dimples does not depend linearly by their number; the dimples is influenced by working conditions and the width of the dimples;
- one of the key parameters appears to be the "aspect ratio", even if it is not possible to uniquely identify an optimum value as this depends actually also by the mutual distance between the dimples

The theoretical model developed is versatile as the main feature in describing different combinations of the basic parameters of the type of the problem studied.

References

[1] I. Etsion, L. Burstein, "A model for Mechanical Seals with Regular Microsurface Structure ", Tribology Transaction, 39, 667-683, 1996.

[2] I. Etsion, Y. Kligerman, G. Halperin, "Analytical and Experimantal Investigation of Laser-Textured Mechanical Seal Faces, Tribology Transaction, 42, 511-516, 1999.

[3] A. Ronen, I. Etsion, Y. Kligerman, "Friction-Reducing Surface Texturing in Reciprocating Automotive Components", Tribology Transaction, 44, 149-158, 2001.

[4] K. Tonder, "Inlet roughness tribodevices: dynamic coefficients and keakage", Tribology International, 34(12), 847-852, 2001.

[5] K. Tonder, "Pivoted inlet texture devices", World Tribology Congress III, 65-6, 2005.

[6] A. Kovalchenko, O. Ajayi, A. Erdemir, G. Fenske, I. Etsion, ''The Effect of Laser Texturing of Steel Surfaces and Speed-Load Parameters on the Transition of Lubrication Regime from Boundary to Hydrodynamic'', Tribology Transaction, 47, 299-307, 2004

[7] S. Cupillard, M.J. Cervantes, S. Glavatskih, " Prssure build-up mechanism in a textured inlet of a hydrodynamic contact", Journal of Tribology, 140, 2008.

[8] V. Brizmer, Y. Kligerman, I. Etsion, " A Laser Surface Textured Parallel Thrust Bearings", Tribology Transaction, 46, 397-403.

[9] S. Cupillard, S. Glavatskih, M.J. Cervantes, "3D Thermohydrodynamic analysis of a textured slider", Tribology Intrnational, 42, 2009.

[10] Y. Kligerman, I. Etsion, "Experimental investigation of Laser Surface Texturing for Reciprocating Automotive Components", Tribology Transaction, 45, 444-449, 2002.

[11] D.B. Hamilton, J.A. Walowit, C.M. Allen " A theory of lubrication by micro-irregularities", ASME J.Basic Eng., 88(1), 177-85, 1996.